Colloid Polym Sci (2003) 282: 56–63
DOI 10.1007/s00396-003-0914-1

ORIGINAL CONTRIBUTION

Gregory S. Watson
Jolanta A. Blach
Colm Cahill
Dan V. Nicolau
Duy K. Pham
Jon Wright
Sverre Myhra

Poly(amino acids) at Si-oxide interfaces—bio-colloidal interactions, adhesion and 'conformation'

Received: 24 October 2002
Accepted: 5 March 2003
Published online: 21 May 2003

G.S. Watson · J.A. Blach · C. Cahill
S. Myhra (✉)
School of Science, Griffith University,
4111 Nathan, Queensland, Australia
E-mail: s.myhra@sct.gu.edu.au
Tel.: +617-3875-7546
Fax: +617-3875-7656

D.V. Nicolau · D.K. Pham · J. Wright
Industrial Research Institute Swinburne,
Swinburne University of Technology,
PO Box 218, 3122 Hawthorn,
Victoria Australia

Abstract Biopolymers in a confined solution environment will be subject to long-range electrostatic and short-range van der Waals interactions. The interactions between two model poly(amino acids), poly-L-lysine and poly-L-glutamic acid, in solution with a Si-oxide surface have been investigated. The model amino acids were adsorbed, or covalently coupled, to colloidal probes consisting of a micro-sphere attached to a force-sensing lever. The methodology was based on sensing interaction between the probe and a flat surface through carrying out force versus distance analysis with a scanning force microscope. The framework of the conventional DLVO theory was used to arrive at a qualitative description. The outcomes illustrate both repulsive and attractive long-range interactions that will hinder, or promote, transport of colloidal biospecies into the region of attractive short-range interactions at the physical interface. Large 'snap-on' distances were observed for some systems and were ascribed to compression of the 'soft' functionalised layers. Those observations and measurements of adhesion provided insights into conformation of the adsorbed species and strength of attachment. The results are relevant to design and functionality of Si-based microfluidics technology.

Keywords Double layer interactions · Poly(amino acids) · Colloidal probe microscopy · DLVO model

Introduction

Adsorption of proteins on solid surfaces has been described as 'a common but very complicated phenomenon' [1]. Complications arise, in part, from geometrical complexity, functional heterogeneity and conformational lability. Systems and processes that fall under the general heading of molecular-scale interactions—e.g. protein folding, growth of biofilms, heterogeneous catalysis, and (bio)chemical separation—respond principally to short-range interactions and steric constraints. In the case of colloidal species in solution, mass transport will respond to electrostatic forces arising from net surface charge densities on the colloid and on its destination surface/interface. The properties of the medium then play important roles, e.g. [2]. The DLVO theory [3] takes account of the diffuse double layer causing action over an intermediate range, as well as the ever-present short-range van der Waals interaction. Recent theoretical modelling has attempted to relate electrostatic interactions to more detailed models of proteins and their confinement [4, 5, 6]. An all-atom calculation of a macromolecule in aqueous solution interacting with a surface is, as yet, not feasible. Thus, it is common practice to consider the molecule as a simplified structure of interconnected subunits, such as amino acids.

The advent of scanning force microscopy (SFM) [7] has provided an important new tool for interrogation of

biomolecular systems; recent work has demonstrated specificity and resolution at the level of single recognition events [8]. Other applications of SFM to investigations of short-range interactions have been reviewed in the literature [9, 10, 11]. On the other hand, the study by SFM of intermediate range interactions in solution between bio-colloids and interfaces has received less attention. The principal aim of the project has been to study interactions of poly(amino acids) in solution with interfaces defined by Si-based technology. The type of analysis, based on colloidal probe, is particularly relevant to micro-bead diagnostics, but the results will also shed light on the characteristics of the sub-units of more complex bio-molecular species.

Electrical double layer and van der Waals interactions

The system consists of a dielectric sphere (the colloidal probe) interacting with a planar surface of a semi-infinite dielectric solid. Both objects have interfaces with, and are submerged in, an aqueous medium. Bound charges will, in general, be present at the interface between the solid and liquid. Boundary conditions require that the effective potential decays exponentially away from the surface at a rate defined by the Debye length, κ^{-1}. At separations >10 nm, an electrostatic interaction arising from the overlap of the double layers will generally dominate over other interactions. At smaller separations, the attractive van der Waals interaction becomes increasingly dominant. In the context of an SFM-based experiment the sphere will be attached to the end of a force-sensing/imposing lever; the force-response of the lever is described by,

$$\Delta F_L = k_N \Delta z_L \tag{1}$$

where k_N is the spring constant corresponding to normal deflection, Δz_L, of the lever. At a separation between sphere and plane of d, the static force imposed by the lever is balanced by electrostatic, F_E, and van der Waals, F_{vdW}, interactions acting on the sphere

$$\Delta F_L(d) = F_E(d) + F_{vdW}(d) \tag{2}$$

The two contributions are conventionally described by the DLVO theory (Derjaguin, Landau, Verway and Overbeek) [12, 13]. In the regime of low surface potentials (i.e. concentration of counterions greater than 1 mM), and when charge regulation has been neglected, the double layer interaction between a sphere and a flat surface can be described by

$$F_E(d) = \left[\frac{4\pi R\sigma_1\sigma_2}{\varepsilon\varepsilon_0\kappa}\right]\exp(-\kappa d) \tag{3}$$

where R is the radius of the sphere, σ_1 and σ_2 are the respective surface charge densities, ε is the relative permittivity of the aqueous medium, and ε_0 is the permittivity of free space. The Debye length is dependent on the concentration and valence of species in the bulk solution, in accord with

$$\kappa^{-1} = \sqrt{\frac{\varepsilon\varepsilon_0 kT}{e^2\sum n_i^{\infty} Z_i^2}} \tag{4}$$

where k is the Boltzmann constant, n_i^{∞} is the concentration of i-type ions in bulk solution and Z_i is the ionic valence. The van der Waals force for the same geometries is given by

$$F_{vdW}(d) = -\frac{HR}{6d^2} \tag{5}$$

with H being the Hamaker constant. The DLVO formalism becomes more complex when the surfaces are terminated by multi-layer structures, with depth-dependent charge distributions, and when conformational dynamics are likely to play a role. The present study has confined itself to using the simple DLVO formalism as a tool for curve-fitting the data, and as an aid in the qualitative interpretation of the results.

A force versus distance (F-d) curve may be plotted with the force imposed/sensed by the lever along the vertical axis, and with the difference between stage travel and lever deflection, ($\delta = \Delta s - \Delta z_L$), plotted along the horizontal axis, referenced to the point of zero net interaction. The 'force constant of interaction', k_i, is then given by the magnitude of the slope of the force curve, i.e.

$$k_i(d) = \left|\frac{dF_L(\delta)}{d\delta}|_{\delta=d}\right| = \frac{k_N\Delta z_L}{|\Delta s - \Delta z_L|}|_d \tag{6}$$

The respective force constants for double layer and van der Waals interactions are

$$k_E(d) = |-\kappa F_E(d)| \tag{7}$$

$$k_{vdW}(d) = \left|-\frac{2F_{vdW}(d)}{d}\right| \tag{8}$$

Some of the SFM-based work has been carried out by sensing forces in the sub-nN range versus distance between a Si or Si_3N_4 tip and a flat surface, e.g. [14]. More often, however, a micro-bead is attached at the location of the tip, so as to produce a 'colloidal' probe; that arrangement has a number of merits for investigations of intermediate-range interactions [15, 16]. The geometry of the probe is then known with greater relative certainty than in the case of the tip; the surface chemistry of a bead can be prepared with greater flexibility and reliability; the greater surface area will amplify the strength of interaction and thus improve the signal-to-noise ratio.

The functional dependence and magnitude of forces and the respective force constants for a silica micro-sphere interacting with a flat silica surface will determine the

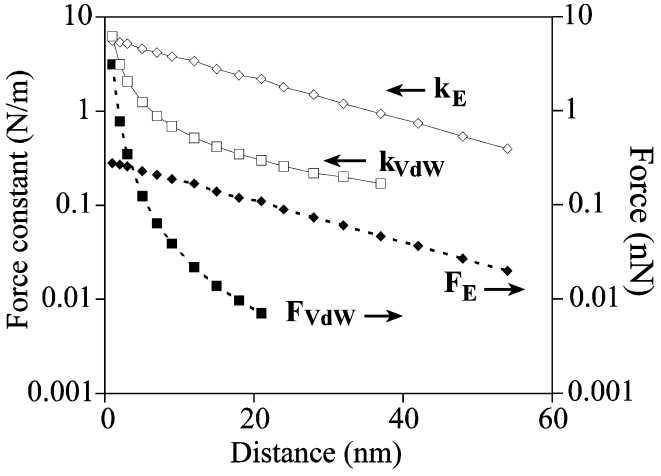

Fig. 1 Magnitudes of generic double layer and van der Waals interactions, and their respective force constants as functions of separation between a silica microsphere and a flat silica surface. The parameters are listed in the text

response of the probe, and are illustrated in Fig. 1 for generic values of parameters and variables. The surface charge densities are taken to be $\sigma_1 = \sigma_2 = 6\times10^{-4}$ C/m^2 [17]. Other parameters include $\kappa^{-1} = 20\times10^{-9}$ m, $R = 2.5\times10^{-6}$ m, $\varepsilon = 80$, and $H = 0.75\times10^{-20}$ J [17]. The response of the lever with a force constant k_N will now depend on the sign of F_E and on the force constant, k_S, corresponding to the sum of the forces acting on the micro-sphere. When $k_S > k_N$, and $F_{vdW} > F_E$, the tip will snap into contact. When the electrostatic interaction is attractive, the lever will always be deflected towards the flat surface, with the van der Waals force playing an increasingly prominent role for small d. Again, when $k_S > k_N$, the tip will snap into contact.

Interacting 'hard' bodies can be assumed to be incompressible. Accordingly the total lever deflection at snap-on, $d_{snap\text{-}on}$, is equal to the separation distance at the point where $k_S = k_N$. Van der Waals interaction is short-range, in comparison with double layer interaction. Thus $F_E(d_{snap\text{-}on} + 1\text{ nm}) \approx k_N(\Delta z_{snap\text{-}on} - d_{snap\text{-}on})$, while $F_{vdW}(d_{snap\text{-}on} - 0.5\text{ nm}) \approx k_N \Delta z_{snap\text{-}on}$, where $\Delta z_{snap\text{-}on}$ is the lever deflection at the point of snap-on. If one or both of the interacting objects are 'soft', as in the case when the surfaces are functionalised with bio-organic species, then $d_{snap\text{-}on}$ will reflect compression/penetration at the point of contact, as well, and is no longer representative of the range of interaction.

Experimental section

Details of materials and probes

An n-type Si wafer with RMS roughness of 0.2 nm covered by a native oxide layer constituted an SiO_2 surface with an iso-electric point, IEP, at a solution pH of ca. 2. It should be noted that a distinction is being made between 'silica' and native oxide on a Si wafer surface. PSMA, poly(styrene-r-malaic-anhydride), having COOH termination as a result of treatment with 1 M NaOH was used as an alternative flat substrate for attachment of poly-L-lysine through EDC coupling.

A V-shaped lever microfabricated from Si_3N_4 with a nominal force constant $k_N = 0.58$ N/m constituted the force-sensing element of the probe. A particular micro-sphere was attached to the lever with the aid of a micromanipulator. The procedure consisted of dipping the tip into a droplet of glue, and then lowering the tip onto a micro-sphere. The geometry and surface structure of the apex of each particular micro-sphere was characterised by 'reverse' imaging [18].

Silica micro-spheres without and with COOH functionalisation were obtained from Bangs Laboratories (S-series and catalogue no. SC05 N, respectively). Polystyrene micro-spheres with NH_2 termination were obtained from Polysciences (catalogue no. 19118). The as-received silica probe was used for procedural validation (e.g. silica versus SiO_2). It should be noted that a silica microbead will not in general present a reproducible and time-invariant surface chemistry, even setting aside the issue of initial cleanliness and the possibility of being contaminated during analysis. The density and structure of surface states will depend on the method of manufacture. More importantly, the surface will undergo aqueous degradation through base catalysed hydrolysis, leading to formation of a silicaceous gel layer. The present experimental strategy aimed at acquiring data during the early stages of aqueous attack, and at reproducing the probe condition from one run to another. Surface functionalisation of the probes provided the means for investigation of interaction between an amino acid and a bioactive surface. The polystyrene/NH_2 probe was used for attachment of poly-L-glutamic acid.

Surface functionalisation

Surfaces were functionalised either by direct adsorption from DDDW solution at pH 5.5–6, or by covalent coupling through EDC, 1-ethyl-3-(dimethylaminopropyl)carbodiimide hydrochloride. Two poly(amino acid) species were investigated in the present study, poly-L-lysine (Sigma P-6282) with 70 kD molecular weight corresponding to an average chain length of ca. 600 units, and poly-L-glutamic acid (Sigma P-4761) with 44 kD and an average chain length of ca. 400 units. Direct adsorption was carried out by immersion of the probe in a solution of 100 μg/mL, followed by a rinse in DDDW in order to remove unbound species. The wet chemical procedure began with immersion of the colloidal probe, with either COOH- or NH_2-termination, in solution (e.g. 10 μL poly-L-lysine at 100 μg/mL plus 0.5 μL 0.1 M EDC) for 30–45 min.

SFM instrumentation and methodologies

The work was carried out with a ThermoMicroscopes TMX-2000 Explorer system fitted with a 130×130 μm^2 scanner. The solution cell consisted of a glass surface on which multiple specimens were located. The active volume of the cell was defined by a large droplet of DDDW. The 'standard' experiments at pH 6 and 11 on interactions between a silica sphere and a flat Si-oxide surface were carried out in an aqueous cell without added salt. However, salt was added at a molar concentration of 10^{-3} to one experiment on silica versus SiO_2 as yet another element of quality control. The open cell allowed the aqueous medium to became fully equilibrated with atmospheric CO_2 giving rise to a pH of 5.8–6. A typical experimental run lasted some 2–4 h.

Given the structural and biochemical complexity of the systems being investigated, in comparison with most previous investigations of DLVO-type systems, a particular strategy was adopted in order to 'boot-strap' parameters from one system to another. Measurement

of the double layer interaction between a silica micro-sphere and an oxidised Si wafer specimen constituted the 'standard' experiment, whereby the surface charge density was determined for silica, and against which the integrity of the probe was validated. Each subsequent step in the analysis involved replacement of just one surface, while the other parts of the system were retained, so that parameters from the previous step could be carried forward. Analysis of all surfaces were carried out in rotation at each successive step with a particular probe within a common aqueous envelope, and with periodic return to the standard experiment, in order to maintain internal consistency, and in order to improve relative discrimination.

An F-d measurement consists of approach and retract half-cycles. The former will reveal the strength of long-range interactions and their functional dependence on separation between probe and surface, as well as the tip-to-surface separation at which the shorter range attractive interactions become dominant. The net change in separation of the sphere from the flat surface is given by the change in z-stage position minus, or plus, lever deflection for repulsive or attractive interactions, respectively ($\Delta d = \Delta s \pm \Delta z_L$). The retract half-cycle will provide information about probe-to-surface adhesion that arises from short-range attractive interactions. The data presented below are representative examples of F-d curves from much larger sets of analyses.

Results and discussion

Standard experiments

Silica probe versus SiO_2 surface

Representative F-d curves showing data for the approach half-cycle for solution pH of 6 and 11, without salt, and for pH 6 with 1 mM added salt, are shown in Fig. 2a–c. Only data from the initial stages of aqueous exposure were considered, in order to avoid effects of silica dissolution and formation of a silicaceous gel layer [19]. The respective Debye lengths, as curve-fitting parameters, were 27 ± 3 and 40 ± 2, for pH 6 and 11 and no salt, and 21 ± 3 nm with 1 mM salt. Those trends are consistent with the trends in concentration of counterions. The curves exhibited the expected repulsive interaction for $d > 5$ nm. At low pH an attractive short-range interaction was manifest by the snap-on feature at a probe-to-surface separation of ca. 3 nm. At the point of snap-on the net force was 2.5–4 nN. Surfaces charge densities of $\sigma_1 = \sigma_2 = -(1.8 \pm 0.3) \times 10^{-3}$ C/m^2 are then required in order to fit the data to the expression for electrostatic repulsion. An attractive van der Waals force will dominate for a probe-to-surface separation marginally less than 2 nm. Treating H as a free parameter we find then that the effective Hamakers constant was $(2.0 \pm 0.5) \times 10^{-20}$ J. At pH 11, the force constant of the electrostatic interaction exceeded that of the lever over the entire range; thus the probe was prevented from entering the force field of the van der Waals interaction. These results are in overall agreement with those obtained in other studies [14, 20].

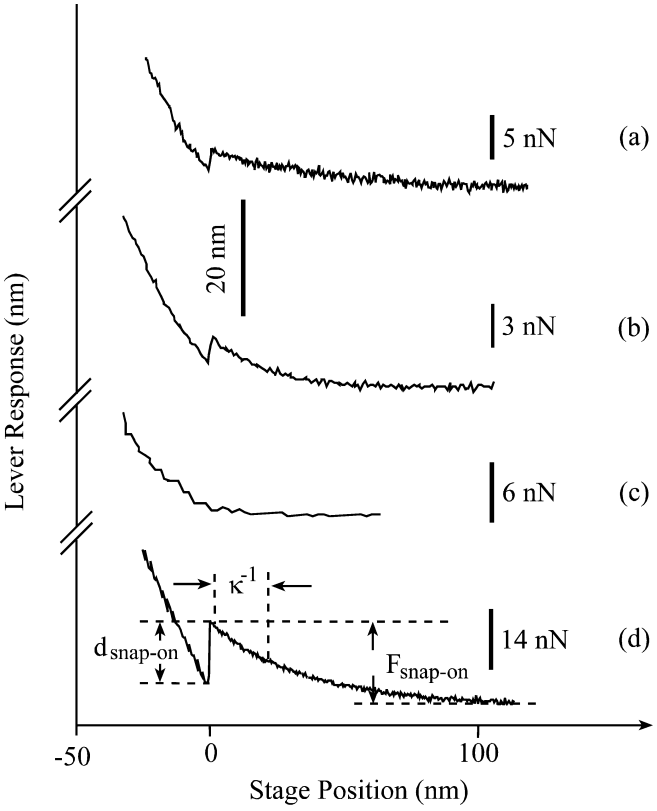

Fig. 2 F-d approach force curves for silica versus SiO_2 at pH 6 (*a*) and 11 (*c*) with no salt, pH 6 with 1 mM added salt (*b*); and for a COOH-terminated silica sphere at pH 6 and no salt (*d*). The individual *vertical scale bars* refer to force being sensed or imposed by the lever; the *vertical distance scale bar* refers to lever deflection; stage travel in the z-direction is plotted along the horizontal axis. The relevant parameters are indicated on *d*

Silica/COOH probe versus SiO_2 surface

It has been shown that COOH groups are substantially deprotonated at pH 6 [10]; thus there will be a negative surface charge on the probe and a repulsive interaction with the SiO_2 surface, Fig. 2d. The Debye length, some 25 nm, was comparable to that of the silica/SiO_2 pairing. However, there was greater strength of electrostatic interaction for COOH termination (ca. 12 nN at the point of snap-on). Accordingly, there is a correspondingly greater effective surface charge density on the COOH terminated surface, $(-4 \pm 2) \times 10^{-3}$ C/m^2, in comparison with the silica probe. The onset of snap-on at an apparent separation of ca. 10 nm shows that a 'soft' layer is being compressed at the point of contact, when the strength of van der Waals interaction exceeds that of electrostatic repulsion. The layer consisted of the coupling agent(s) and COOH-termination of the silica sphere. Assuming that the layer was effectively compressed to near-zero thickness, it can be inferred that the maximum extent of the layer in water was ca. 8 nm.

Since the separation at the point when $F_{vdW} > F_E$ is ill-defined, then the Hamaker constant cannot be determined for this particular system.

Interactions with amino acids

Silica/poly-L-lysine probe versus SiO_2 surface

The F-d curves at pH 6 for a SiO_2 surface are shown in Fig. 3c. An attractive interaction is evident, with $\kappa^{-1} \approx 30$ nm, and a strength of 6 ± 2 nN at the point where the snap-on occurred; the snap-on distance was ca. 5 nm and the adhesive interaction was ca. 25 nN. At pH 6 the amine group on the side-chain should be protonated and will present a positive charge; an IEP of 10.5 has been reported [21]. Hence, the species is readily adsorbed onto silica. However, it has been shown that due to conformational hindrance only one in eight mid-chain segments will attach to a silica surface [22]. Thus the functionalised probe will present an effective positive surface charge density, inferred from Eq. 3 to be $(2.5 \pm 0.5) \times 10^{-3}$ C/m^2. Since the double layer interaction is attractive, then snap-on will now take place at a separation of some 5 nm, when the effective force constant of interaction exceeds that of the lever. Given that the layer of poly-L-lysine is compressible, the snap-on distance will represent extent of deformation at the point of contact, plus the range of van der Waals interaction. A compression of 3–4 nm is consistent with monolayer coverage of the colloidal probe, on average, and with the lysine having undergone unfolding during attachment to the probe. The length of a lysine monomer is reported as 0.79 nm [22], and modelling suggests that poly-L-lysine adsorbed onto silica glass will adopt a helical configuration with every eighth monomer being hydrogen bonded. The approximate diameter of the helix is thus 2 nm, in reasonable agreement with the present data. The condition of $k_S > k_N$ will pertain at a separation of marginally less than 5 nm, at which point the probe will snap into contact. The upper limit on H was then $(3 \pm 1) \times 10^{-20}$ J, if the attraction at $d \approx 1.5$ nm is ascribed to van der Waals interaction. The value for H is in reasonable agreement with results of other studies [23].

The retract curve exhibited a force of adhesion of ca. 25 nN. That force should be representative of interactions between the lysine monomers and the flat SiO_2 surface. However, release may arise at either of the two interfaces between silica/SiO_2 and poly-L-lysine.

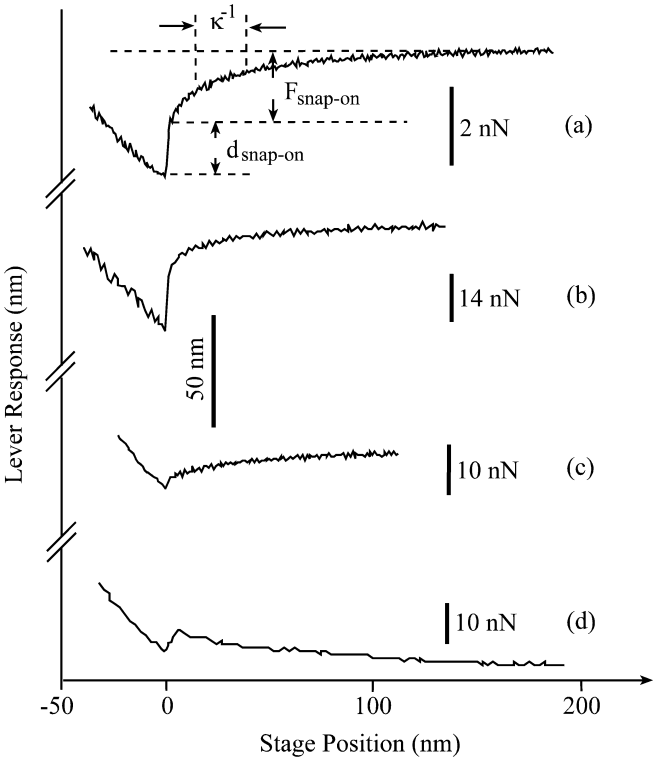

Fig. 3 F-d approach force curves for interaction of poly(amino acids). (*a*) Lysine adsorbed via EDC coupling onto a COOH-terminated silica sphere versus an SiO_2 surface. (*b*) Glutamic acid adsorbed via EDC coupling to an NH_2-terminated polystyrene sphere versus lysine attached via EDC coupling to a PSMA polymer surface. (*c*) Lysine adsorbed onto a silica sphere versus an SiO_2 surface. (*d*) Glutamic acid attached via EDC coupling to an NH_2-terminated polystyrene sphere versus an SiO_2 surface. The individual *vertical scale bars* refer to the force being sensed/imposed by the lever; the single *vertical distance scale bar* refers to lever deflection; stage travel in the z-direction is plotted along the horizontal axis. The relevant parameters are defined on curve (*a*)

Silica/COOH(EDC)/poly-L-lysine probe versus SiO_2 surface

The amino acid was now adsorbed via EDC coupling, with the objective of generating covalent attachment. The force curves are shown in Fig. 3a. The Debye length was now some 30 nm; the strength of interaction at the point where snap-on occurred was 2.5 ± 1 nN, while the snap-on distance was 22 ± 5 nm, and force of adhesion was ca. 85 nN. The results indicate that the net positive surface charge density was lower, $(1.3 \pm 0.4) \times 10^{-3}$ C/m^2, when attachment was effected by COOH termination, as opposed to adsorption to a bare silica surface. One might speculate that the greater conformational freedom of COOH functionalisation will allow additional bonding to poly-L-lysine and, thus, greater charge compensation. The adhesion was considerably higher than in the case of adsorption to silica, and the snap-in distance of 22 ± 5 nm was greater than that, 10 ± 3 nm, observed for the COOH-functionalised probe interacting with a flat SiO_2 surface. Those results suggest that the lysine forms a bilayer with the COOH-functionalised layer. At sphere-to-flat contact the lysine will be confined in a silica-COOH(EDC)/lysine-SiO_2 sandwich. The bonding of lysine

to COOH should be the strong link in the chain. During retraction it is therefore plausible to ascribe the release mechanism to separation at sites of attachment of the lysine chain at the flat interface.

Polystyrene/NH_2(EDC)/Poly-L-glutamic probe versus SiO_2 surface

Poly-L-glutamic acid was attached to the probe through EDC coupling to an NH_2-terminated polystyrene micro-sphere. NH_2-termination is likely to generate a positive surface charge at pH 6. Poly-L-glutamic acid, on the other hand, is likely to present negatively charged sites at that pH. The F-d data, Fig. 3d, revealed weak repulsive interaction with the SiO_2 surface with $\kappa^{-1} = 60$–80 nm while the repulsive force at snap-on was 8 ± 3 nN and the snap-in distance was 10 ± 4 nm. The data suggest, as in the case of attachment of poly-L-lysine, that only some of the mid-chain sites were attached to the sphere, and that there was a net negative surface charge on the probe. The estimated surface charge density was -1.5×10^{-3} C/m^2, but the large value of κ^{-1} in combination with poor force resolution, would suggest that the results must be treated with some caution. The strength of adhesion, some 3 nN, was consistent with weak interaction, leading to only slight compression and a small contact area. The net negative charge on the probe may be distributed throughout the thickness of the adsorbed layer, thus promoting a lower force of adhesion.

Poly-L-glutamic probe versus poly-L-lysine surface

Poly-L-lysine was adsorbed onto a PSMA surface via EDC coupling. A polystyrene probe with NH_2-termination functionalised through EDC coupling with poly-L-glutamic acid was then prepared, in order to confirm the charge states of the separate attachment schemes for the biospecies. The expected attractive interaction was evident, Fig 3b, with a $\kappa^{-1} \approx 21$ nm, and a characteristic strength of interaction of 15 ± 5 nN at the point of snap-on. The charge density for the surface functionalised with lysine was taken as 2.5×10^{-3} C/m^2; the inferred charge density on the surface functionalised with glutamic acid turned out to be ca. -4×10^{-4} C/m^2. *Thus there is moderately good internal self-consistency*. The snap-on distance was ca. 20 nm. The strength of adhesion was ca. 30 nN, again reflecting compression of 'soft' layers at the probe-to-surface point of contact.

Compression and adhesion

In the ideal case of two atomically flat and incompressible surfaces coming together, the snap-on distance essentially represents the range of attractive interactions.

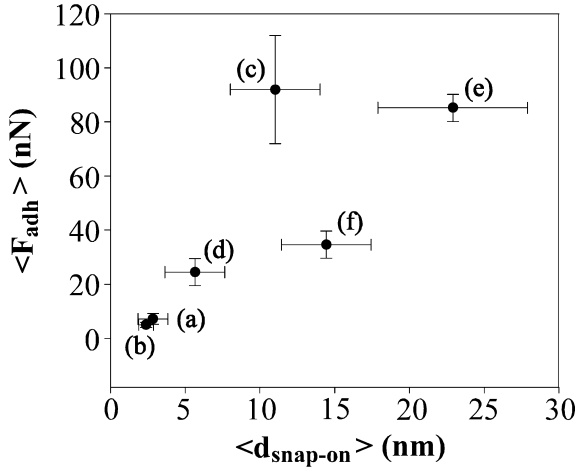

Fig. 4 Average snap-on distance versus average adhesion for the combinations of probe and surface investigated in the present study. The labels refer to: (*a*) Silica vs. SiO_2; (*b*) silica vs. Y_2O_3; (*c*) silica/COOH vs. SiO_2; (*d*) silica/lysine vs. SiO_2; (*e*) silica/COOH/lysine vs. SiO_2; (*f*) polystyrene/NH_2/glutamic vs. SiO_2/lysine. The data for Y_2O_3 represents a system where the surface charge density is positive at pH 6, and has been included for comparison

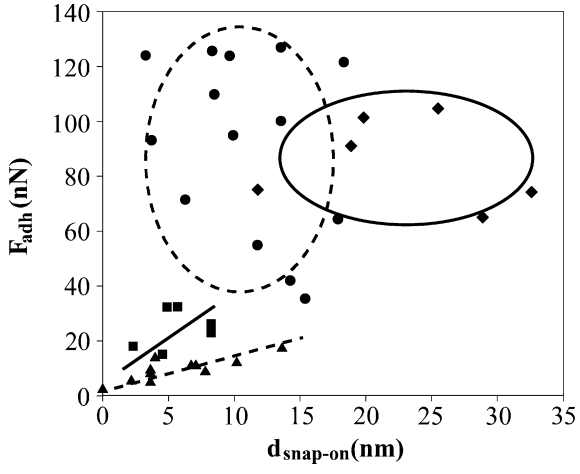

Fig. 5 Representative data for adhesion of a COOH functionalised probes with a SiO_2 flat surface, ●, do not scale with contact area. The data are grouped by a *broken line*. However, adhesion for silica and silica/lysine probes does appear to scale with contact area; the data points are denoted by ▲·and ■·symbols, respectively. The data for COOH/lysine functionalisation, ♦, are included for comparison. They fall on the trend, on average, but with considerable scatter (and are grouped by a *solid line*)

The adhesive force should then be substantially proportional to the contact area, if short-range interface interactions dominate over other net attractive forces. A silica micro-sphere interacting with a flat silica surface is a close approximation to the ideal case. In practice the ideal case cannot be fully realised due to topographical irregularities, transfer of material to/from the probe apex, lateral differentiation in surface chemistry of probe and/or surface, etc.

When one or both of the surfaces are functionalised, there will be compression of the 'soft' interfacial layer, as manifested by a longer snap-on distance, and by additional adhesion due to the correspondingly larger contact area. Extent of compression/indentation by an object of parabolic shape, equivalent to a spherical section at the apex of the probe, is related to Young's modulus, E, of the 'soft' material, the applied load, $F = F_{adh} \pm k_N \Delta L$, and the radius of curvature of the probe. The relevant expression is, e.g. [24].

$$E = \frac{3F(1-\mu^2)}{4\sqrt{R}\Delta z^{3/2}} \quad (9)$$

where μ is Poisson's ratio (generally in the range 0.3–0.5). Taking representative values for $F = 50$ nN, $R = 2.5$ μm, $\mu = 0.5$ and $\Delta z = 10$ nm, the corresponding value of E is 20 MPa. The rationale for the calculation is to show that if Young's modulus for the 'soft' material is less than 20 MPa, then there will be a compression of 10 nm for a force of attraction of 50 nN acting on the probe. Accordingly, there is justification for the argument that large values of snap-on distances represent compression. Values for E in the range 1–20 MPa have been measured for lipid layers on wool fibre [25], polyurethane [26], rubber and gelatin [27]. The effect on total force loading of the lever-imposed force will be negligible, if $k_N d_{snap\text{-}on} << F_{adh} = k_N d_{lift\text{-}off}$. The measurements described above will satisfy that condition.

Additional information about the system can be extracted from the data. Figure 4 shows the average adhesion as a function of average snap-on distance for combinations of probe and flat surface. The area of a spherical segment of height d is given by 2π Rd. Thus, $d_{snap\text{-}on}$ is directly proportional to the contact area when a deformable layer is compressed between a sphere and flat surface, where the extent of compression is given by $d_{snap\text{-}on}$ minus the range(s) of the attractive interaction(s) at the point of snap-on. For $R = 2.5$ μm an indentation/compression of 10 nm will correspond to a contact area of 1.6×10^5 nm^2. A line of best fit of the data in Fig. 4 corresponds to the zeroth order approximation that the adhesion is proportional to the contact area irrespective of the structure or chemistry of the interfaces. The average adhesion per unit area is then 0.25 pN/nm^2 (corresponding to a tensile strength of 0.25 MPa). The values for the COOH-functionalised probes, without adsorbed lysine, fall significantly above the trend line, while the interaction between the glutamic and lysine surfaces falls marginally below. Further examination of the data revealed that those values for average adhesion that conformed to the trend also tended to obey the rule that adhesion was proportional to contact area. On the other hand, the combination with average adhesion that was above the trend line disobeyed the rule. The data in Fig. 5 illustrate the former case for silica and silica/lysine versus SiO_2, and the latter case for silica/COOH versus SiO_2. A likely

Table 1 Representative results from colloidal probe analysis

System	Salt (mM)	κ^{-1} (nm)	$F_{snap\text{-}on}$ (nN)	$d_{snap\text{-}on}$ (nm)	F_{adh} (nN)
Silica vs. SiO_2 (pH 6)	No	27 ± 3	4 ± 1	2.5 ± 1	5 ± 2
Silica vs. SiO_2 (pH 6)	1	21 ± 3	3.5 ± 1	4 ± 1	20 ± 10
Silica vs. SiO_2 (pH 11)	No	40 ± 2	na	na	na
Silica/COOH vs. SiO_2	No	25 ± 4	12 ± 3	10 ± 3	90 ± 20
Silica/lysine vs. SiO_2	No	30 ± 3	6 ± 2	5 ± 2	25 ± 5
Silica/COOH(EDC)/lysine vs. SiO_2	No	30 ± 4	2.5 ± 1	22 ± 5	85 ± 5
Polystyrene/NH_2(EDC)/glutamic vs. SiO_2	No	60–80 (?)	8 ± 3	10 ± 4	3 ± 1
Polystyrene/NH_2(EDC)/glutamic vs. PSMA(EDC)/lysine	No	21 ± 2	15 ± 5	20 ± 5	30 ± 5

The result marked with a question mark does not fit the expected trends, but has been included for completeness. See additional comments in the text

Table 2 System characteristics inferred from application of DLVO analysis

System	σ_1 (C/m^2)	σ_2 (C/m^2)	κ^{-1} (nm)	H_{eff} (10^{-20} J)
Silica vs SiO_2	$-(1.8 \pm 0.3)\times10^{-3}$	$-(1.8 \pm 0.3)\times10^{-3}$	27	2.0 ± 0.5
Silica/COOH vs SiO_2	$-(4 \pm 2)\times10^{-3}$	$-(1.8 \pm 0.3)\times10^{-3}$	25	na
Silica/lys vs SiO_2	$(2.5 \pm 0.5)\times10^{-3}$	$-(1.8 \pm 0.3)\times10^{-3}$	30	2 ± 1
Silica/COOH/lys vs SiO_2	$(1.3 \pm 0.4)\times10^{-3}$	$-(1.8 \pm 0.3)\times10^{-3}$	30	3 ± 1.5
Polystyrene/NH_2/glut vs SiO_2	$-(1.5 \pm 0.5)\times10^{-4}$ (?)	$-(1.8 \pm 0.3)$v10^{-3}	60–80 (?)	na
Polystyrene/NH_2/glut vs SiO_2/lys	$-(4 \pm 2)\times10^{-4}$	$(2.5 \pm 0.5)\times10^{-3}$	21	na

The results marked with a question mark do not fit the expected trends, but have been included for completeness. See additional comments in the text

explanation is that of hydrogen bonding between deprotonated COOH species on the probe and hydroxyl species on the surface. When lysine is adsorbed onto the functionalised probe, the effect is to occupy some of the otherwise available COO^- sites and/or render them sterically hindered.

The experimental results of the study have been summarised in Table 1. As well as considering the features of the approach curves from F-d analysis by colloidal probes, the shorter range adhesive interactions (i.e. lift-off force in the retract curve) have been tabulated. One must be cautious in attaching too much importance to the latter entries, however, since they depend on the actual contact area and on the local surface density of interacting species. Results inferred from application of the standard DLVO framework to the data are summarised in Table 2.

The double-layer will effectively constitute a potential well, or barrier, anchored to the interface, as seen by a bio-colloid in bulk solution. The shape of the well, or barrier, is determined principally by the charge density at the interface; concentration, valence, polarity and distribution of counter-ions and co-ions in solution; the IEP of the surface and the colloid, and the local pH; local dielectric constant; and temperature. The depth of the well, or height of the barrier, is often large in comparison with k_BT. Accordingly Brownian motion cannot be relied upon to override the constraints imposed by the well/barrier.

The double layer force on a bio-colloid in solution can readily be estimated from Eq. 3. Taking generic values for the surface charge densities, and setting $d = \kappa^{-1} = 10$ nm, a spherical colloid of radius $R = 10$ nm will experience a force, F_E, of ca. 1 pN. The aqueous phase may now be taken to be a Stokes fluid. Taking the force to be 1 pN, it is apparent that velocities of $\approx 5 \times 10^{-3}$ m/s will arise from double layer interactions. Such a velocity is significant in the context of fluid flow in microfluidics devices.

Conclusions

The study shows that the colloidal probe implemented on an SFM platform constitutes a convenient and informative method of investigating interactions arising from confinement of biomolecular species in solution. The system and its characteristics are relevant to fundamental insights as well as technological applications.

The outcomes have implications for devices and processes that are affected by static and dynamic properties of micro/nano-fluidic confinement of bio-colloids. The impact may constitute a threat, but may also provide opportunities. For instance, it has been demonstrated that bio-colloids can be adsorbed selectively from solution by adjustment of ions in solution and/or pH [28]. Until the arrival of the next generation of computational packages, experiments such as those described above will be required in order to predict and validate functionality.

Acknowledgements The work was supported in part by a US DOD DARPA grant No. F30602-00-2-0614.

References

1. Nakanishi K, Sakiyama T, Imamura K (2001) J Biosci Bioeng 91:233
2. Fröberg JC, Rojas OJ, Claesson PM (1999) Int J Miner Process 56:1
3. Israelachvili JN (1991) Intermolecular and surface forces. Academic Press, London
4. Roth CM, Sader JE, Lenhoff AM (1998) J Colloid Interface Sci 203:218
5. Asthagiri D, Lenhoff AM (1997) Langmuir 13:6761
6. Sader JE, Chan DYC (2000) Langmuir 16:324
7. Binnig G, Quate CF, Gerber C (1986) Phys Rev Lett 56:930
8. Hinterdorfer P, Baumgartner W, Gruber HJ, Schilcher K, Schindler H (1996) Proc Natl Acad Sci USA 93:3477
9. Willemsen OH, Snel MME, Cambi A, Greve J, de Groot BG, Figdor CG (2000) Biophys J 79:3267
10. Takano H, Kenseth JR, Wong S-S, O'Brien JC, Porter MD (1999) Chem Rev 99:2845
11. Van der Vegte EW, Hadziioannou G (1997) Langmuir 13:4347
12. Derjaguin BV, Landau L (1941) Acta Physicochem URSS 41:633
13. Verway EJW, Overbeek JThG (1948) In: Theory of the stability of lycophobic colloids. Elsevier, New York
14. Senden TJ, Drummond CJ (1995) Colloids Surf A 94:29
15. Ducker WA, Senden TJ, Pashley RM (1991) Nature 353:239
16. Giesbers M, Kleijn JM, Fleer GJ, Cohen Stuart MA (1998) Colloids Surf 142:343
17. Squires T, Brenner MP (2000) Phys Rev Lett 85:4976
18. Hellemans L, Waeyaert K, Hennau F (1991) J Vac Sci Technol B9:1309
19. Adler JJ, Rabinovich YI, Moudgil BM (2001) J Colloid Interface Sci 237:249
20. Hartley PG, Larson I, Scales PJ (1997) Langmuir 13:2207
21. Afshar-Rad T, Bailey AI, Luckham PF (1988) Colloids Surf 31:125
22. West JK, Latour R, Hench LL (1997) J Biomed Mater Res 37:585
23. Bowen WR, Hilal N, Lovitt RW, Wright CJ (1998) J Colloid Interface Sci 197:348
24. Blach JA, Watson GS, Busfield WK, Myhra S (2001) Polym Int 51:12
25. Crossley JAA, Gibson CT, Mapledoram LD, Huson MG, Myhra S, Pham DK, Sofield CJ, Turner PS, Watson GS (2000) Micron 31:659
26. Weisenhorn AL, Khorsandi M, Kasas S, Gotzos V, Butt H-J (1993) Nanotechnology 4:106
27. Radmacher M, IEEE Engng Med Biol (1997) March/April: 47
28. Müller DJ, Amrein M, Engel A (1997) J Struct Biol 119:172